

Laser- and collision-induced nonadiabatic wave-packet dynamics in sodium molecules

F. Grossmann¹, U. Saalman², and R. Schmidt¹

¹Institut für Theoretische Physik, Technische Universität Dresden, D-01062 Dresden, Germany

²Atomfysik, Stockholms Universitet, Frescativägen 24, S-10405 Stockholm, Sweden
frank@physik.tu-dresden.de

Received 30 June 2000, accepted 19 July 2000

Abstract. We investigate nonadiabatic dynamics of molecular sodium in two alternative approximate ways. Firstly, the semiclassical mapping formalism is used to study the decisive step in resonant two photon ionization of Na₂, where the Rabi oscillations of the occupation probability of the resonantly excited intermediate state are reproduced with a high degree of accuracy. Secondly, nonadiabatic quantum molecular dynamics is combined with the surface hopping approach of Tully in order to take into account quantum effects on the nuclear dynamics in collisionally excited sodium molecular ions. Their importance is demonstrated by comparing the results with experimental fragment correlations of kinematically complete experiments.

Keywords: nonadiabatic dynamics, semiclassical wave-packet propagation, molecular dynamics

PACS: 33.80.Be, 03.65.Sq

1 Introduction

The theoretical description of nonadiabatic processes in complex molecular systems is still one of the most demanding problems in atomic many-body theory. In principle it requires the rigorous numerical solution of the full time-dependent Schrödinger equation for the coupled nuclear and electronic dynamics, which has been achieved so far for diatomic (one electron) systems like H₂⁺ excited by a laser field [1, 2]. Obviously, approximate solutions or methods are required in order to deal with more complex systems. On the other hand, any approximate approach has its favorite field of application. Even in simple diatomic molecules, very different types of nuclear wave packet propagation can occur owing to different electronic excitation mechanisms. In this contribution, we will put forth two novel and alternative methods to describe nonadiabatic nuclear wave packet dynamics for laser-driven and collisionally excited sodium molecules, respectively. Both situations have been studied extensively also in corresponding experiments [3–5].

In section 2, the semiclassical implementation of the mapping formalism to nonadiabatic dynamics [6] is applied to the laser pulse driven Na₂ system. The multiphoton

ionization of this system with a short and intense laser pulse has already been calculated quantum mechanically for two photon excitation [7]. Here, semiclassical results for the first step in the excitation process will be compared to numerical quantum results and to approximate analytical Rosen-Zener results for a range of different pulse strengths. In section 3, the so-called non-adiabatic quantum molecular dynamics (NA-QMD) approach [8] is extended, in order to take into account quantum effects on the nuclear dynamics by combining it with the surface hopping mechanism of Tully [9]. As a first application of this method, experimental fragment correlations in kinematically complete experiments of $\text{He}+\text{Na}_2^+$ collisions are analyzed. It is clearly shown that the non-adiabatic nuclear wave packet dynamics leads to pronounced structures in the final fragment distributions. Finally, in section 4, we give conclusions and an outlook on future activities.

2 Laser induced nonadiabatic dynamics

2.1 Semiclassical mapping formalism

In this section we will focus on the nuclear dynamics on two *adiabatic* potential energy surfaces, $U_1(Q)$ and $U_2(Q)$, which are coupled through ultrashort laser pulses of center frequency Ω and with a pulse envelope giving a time dependence to the radiative dipole coupling $V(Q, t)$. Within the rotating wave approximation, the laser field has two effects. First, it leads to a relative overall shift of $\hbar\Omega$ of the two surfaces and second it introduces a coupling of the dynamics on the adiabatic surfaces thus leading to the coupled channel Schrödinger equations

$$\begin{aligned} i\hbar\dot{\Psi}_1(Q, t) &= \left[-\frac{\hbar^2}{2\mu} \frac{\partial^2}{\partial Q^2} + U_1(Q) \right] \Psi_1(Q, t) + V(Q, t)\Psi_2(Q, t) \\ i\hbar\dot{\Psi}_2(Q, t) &= \left[-\frac{\hbar^2}{2\mu} \frac{\partial^2}{\partial Q^2} + U_2(Q) - \hbar\Omega \right] \Psi_2(Q, t) + V(Q, t)\Psi_1(Q, t) \end{aligned} \quad (1)$$

with reduced mass μ .

The quantum mechanical 2×2 Hamiltonian matrix corresponding to the system of equations (1) can now be mapped onto a continuous Hamiltonian [6], whose classical counter part is of the form

$$H(\vec{x}, \vec{p}, Q, P) = \frac{P^2}{2\mu} + H_{\text{el}}, \quad (2)$$

with the momentum P of the nuclear degree of freedom and the “electronic” Hamiltonian

$$H_{\text{el}} = \sum_{i=1}^2 V_{ii}(Q) \frac{1}{2} (x_i^2 + p_i^2 - 1) + \sum_{i < j=1}^2 V_{ij}(Q) (x_i x_j + p_i p_j), \quad (3)$$

where the diagonal matrix elements $V_{ii}(Q)$ are *adiabatic* (shifted) potential energy surfaces $U_1, \tilde{U}_2 = U_2 - \hbar\Omega$ and the nonadiabatic coupling is mediated by the time-dependent offdiagonal matrix element $V_{12}(Q, t) = V(Q, t)$. The vectors $\{x_i\}, \{p_i\}$

denote the canonically conjugate phase space variables corresponding to the continuous harmonic degrees of freedom, representing the discrete two level system.

An approximate solution of the quantum dynamics corresponding to the mapping Hamiltonian can be obtained by using the semiclassical initial value representation (IVR) of the propagator of Herman and Kluk [10]. That this is possible also for driven systems has been shown in a case study on two model potential surfaces (quadratic and linear) [11]. The classical equations of motion for the nuclear degree of freedom entering the semiclassical expression are

$$\dot{Q} = \frac{P}{\mu} \quad (4)$$

$$\dot{P} = - \left(N_1 \frac{\partial U_1}{\partial Q} + N_2 \frac{\partial \tilde{U}_2}{\partial Q} + (x_1 x_2 + p_1 p_2) \frac{\partial V(t)}{\partial Q} \right), \quad (5)$$

with the functions $N_i = (x_i^2 + p_i^2 - 1)/2$ corresponding to the occupation number operators. Using the quantal conservation of probability, one can obtain alternative forms of the classical equations of motion, which might turn out to be favorable if approximations (like the semiclassical IVR methodology) are used. In the simple case of a quadratic coupled to a linear surface, it was not necessary to use this trick. In the numerical investigation of coupled Morse oscillator potentials, to be presented in the following, the equations are highly nonlinear (through the nonlinearity of the Morse forces in addition to the coupling between the nuclear and “electronic” degrees of freedom) and it turned out to be favorable to use a modified Hamiltonian.

2.2 Results for Na_2 driven with a pulsed 345nm laser

The motivation behind the investigations in this section is the question if the semiclassical mapping formalism can be applied successfully to a *realistic* driven molecular system. In order to answer this question we will concentrate on the two-photon ionization of Na_2 . The decisive step in the ionization of Na_2 from the ground ($1^1\Sigma_g^+$) state to the ionization continuum is the population of an intermediate ($2^1\Sigma_u^+$) state via irradiation of the system with a laser pulse of central wavelength 345 nm. We therefore investigate the nonadiabatic dynamics in the ground and intermediate states, which are modelled by Morse function potentials with parameters taken from the spectroscopic data given in Table IV of [12]^a. The dipole moment coupling the two states is taken to be constant (Condon approximation) at a value of 3.7 a.u. Within first order perturbation theory, the ionization probability can then be extracted from the wavefunction on the intermediate potential energy surface [7]. We do not perform the final step in this paper, however.

As the initial state for the dynamics serves the Gaussian approximation to the nuclear ground state wave function of the ground electronic state. The intensity of the laser pulse is varied in the range between about 10^{10} and $2 \cdot 10^{11}$ W/cm². Results for the occupation probability of the intermediate state for three different intensities with

^a in the intermediate state only one single minimum corresponding to the inner minimum of the $2^1\Sigma_u^+$ state is considered

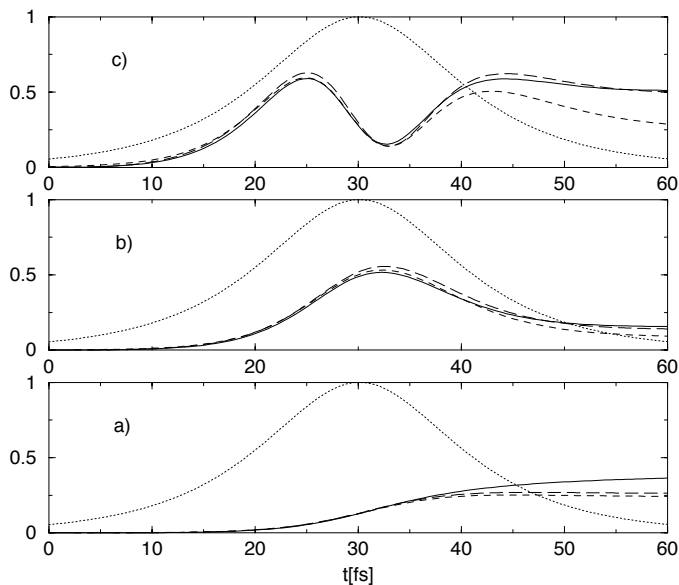


Fig. 1 Comparison of quantum (long dash) Rosen-Zener (short dash) and semiclassical (full line) results for the transfer of probability to the intermediate potential surface for three different laser intensities (a) $9.3 \cdot 10^9 \text{ W/cm}^2$, b) $5.8 \cdot 10^{10} \text{ W/cm}^2$, c) $23.3 \cdot 10^{10} \text{ W/cm}^2$). The (normalized) pulse envelope is indicated by the dotted line.

the same pulse envelope of sech-type and a pulse width of 22 fs are presented in Fig. 1. Here we compare numerical quantum results obtained with the split operator fast Fourier transform method ^b (long dash), approximate Rosen-Zener [14] results (short dash) and semiclassical IVR results (full line). The Rosen-Zener results have been obtained according to Eq. (18) with the integrand replaced by Eq. (17) in Ref. [15].

The agreement between the semiclassical result (which is normalized, in order to conserve the total probability) and the quantum result is striking. For higher intensities, where the probability performs Rabi oscillations, this agreement is even better than the one which can be achieved with the Rosen-Zener approximation.

3 Collision induced dissociation dynamics

3.1 Tully formalism coupled with NA-QMD

We start by summarizing the equations of motion of the NA-QMD approach [8] which comprises equations for the time-dependent Kohn-Sham functions $\psi^j(\mathbf{r}, t)$ and Newton equations for the nuclear coordinates \mathbf{R}_A . Using basis representations $\psi^j(\mathbf{r}, t) =$

^b using exact diagonalization to form the exponential of the 2×2 potential matrix [13].

$\sum_{\alpha} \phi_{\alpha}(\mathbf{r}, \mathbf{R}) a_{\alpha}^j(t)$ they read

$$\dot{a}_{\alpha}^j(t) = - \sum_{\beta\gamma} (S^{-1})_{\alpha\beta} \left\{ iH_{\beta\gamma} + \sum_{A=1}^{N_n} \dot{\mathbf{R}}_A \mathbf{R}_{\beta\gamma}^A \right\} a_{\gamma}^j(t) \quad (6)$$

with $j = 1 \dots N_e$, N_e the number of electrons and

$$\begin{aligned} M_A \ddot{\mathbf{R}}_A = & - \frac{\partial}{\partial \mathbf{R}_A} \sum_{B=1}^{N_n} \prime \frac{Z_A Z_B}{|\mathbf{R}_A - \mathbf{R}_B|} \\ & - \sum_{j=1}^{N_e} \left\{ \sum_{\alpha\beta} \bar{a}_{\alpha}^j \left(\frac{\partial}{\partial \mathbf{R}_A} H_{\alpha\beta} - \left\langle \phi_{\alpha} \left| \frac{\partial}{\partial \mathbf{R}_A} (V_{\text{eff}} - V) \right| \phi_{\beta} \right\rangle \right) a_{\beta}^j \right. \\ & \left. - \sum_{\alpha\beta\gamma\delta} \left[\bar{a}_{\alpha}^j H_{\alpha\beta} (S^{-1})_{\beta\gamma} \mathbf{R}_{\gamma\delta}^A a_{\delta}^j + \text{c.c.} \right] \right\} \end{aligned} \quad (7)$$

with $A = 1 \dots N_n$, N_n the number of nuclei and where \bar{a}_{α}^j is the complex conjugate of a_{α}^j . The matrices in Eqs. (6) and (7) are defined as: $S_{\alpha\beta} \equiv \langle \phi_{\alpha} | \phi_{\beta} \rangle$, $H_{\alpha\beta} \equiv \langle \phi_{\alpha} | \hat{t} + V_{\text{eff}} | \phi_{\beta} \rangle$, and $\mathbf{R}_{\alpha\beta}^A \equiv \langle \phi_{\alpha} | \partial \phi_{\beta} / \partial \mathbf{R}_A \rangle$ with $\langle \dots \rangle$ denoting integration over the single-particle coordinate \mathbf{r} . In these equations \hat{t} is the single particle kinetic energy operator, V denotes the interaction potential of nuclei and electrons and V_{eff} is the effective potential of time-dependent density functional theory using the adiabatic local density approximation [16]. Within the NA-QMD the set of coupled equations (6) and (7) has to be solved simultaneously describing a selfconsistently coupled electron/nuclear dynamics.

In order to treat the coupled dynamics by a surface hopping approach in the sense of Tully [9], the forces on the nuclei determined by the electrons in a certain excited state (potential energy surface) are required. For their determination we use single-particle excitations in the Kohn-Sham picture which are shown to be well-defined approximations for the real excitation energies [17]. The corresponding classical equations then read [8]

$$\begin{aligned} M_A \ddot{\mathbf{R}}_A = & - \frac{\partial}{\partial \mathbf{R}_A} \sum_{B=1}^{N_n} \prime \frac{Z_A Z_B}{|\mathbf{R}_A - \mathbf{R}_B|} \\ & - \sum_{n=1}^{N_e} f_n^K(t) \left\{ \sum_{\alpha\beta} C_{n\alpha} \left(\frac{\partial}{\partial \mathbf{R}_A} H_{\alpha\beta} - \varepsilon_n \frac{\partial}{\partial \mathbf{R}_A} S_{\alpha\beta} \right) C_{\beta n} \right. \\ & \left. - \sum_{\alpha\beta} C_{n\alpha} \left\langle \phi_{\alpha} \left| \frac{\partial}{\partial \mathbf{R}_A} (V_{\text{eff}} - V) \right| \phi_{\beta} \right\rangle C_{\beta n} \right\} \end{aligned} \quad (8)$$

with ε_n and $C_{\beta n}$ or $\phi_n(\mathbf{r}, \mathbf{R}) = \sum_{\beta} \phi_{\beta}(\mathbf{r}, \mathbf{R}) C_{\beta n}$, respectively, the solutions of the secular equations $\sum_{\beta} (H_{\alpha\beta} - \varepsilon_n S_{\alpha\beta}) C_{\beta n} = 0$ at the current positions \mathbf{R}_A . The set f_n^K of occupation numbers (0, 1, or 2) characterizes the electronic state K . The

time dependence of these factors (which consists in sudden hoppings $K \rightarrow K'$) mimics electronic transitions. The determination of these hopping points is done in close analogy to the “fewest switches” procedure by Tully [9].

Let us assume that K is the current electronic state (which governs the classical dynamics) and the Kohn-Sham equations (6) are solved using (automatically adapted) time steps δt , i.e. the coefficients a_α^j are known for certain times. Then at these times, we can generate a sequence of values

$$G_{K'} = \sum_{L=1}^{K'} \frac{B_{KL}}{A_{KK}} \Delta t \quad (9)$$

with $K' = 1 \dots N_s$, where N_s is the number of all possible states accessible by one-particle excitations from state K . The quantities

$$A_{KL} := \det \left\| \sum_{\alpha\beta} C_{n_K\alpha} S_{\alpha\beta} a_\beta^j \right\| \det \left\| \sum_{\alpha\beta} \bar{a}_\alpha^j S_{\alpha\beta} C_{\beta n_L} \right\| \quad (10)$$

$$B_{KL} := -2 \operatorname{Re} \left(A_{KL} \left\langle \phi_{n_K} \left| \frac{\partial}{\partial t} \phi_{n_L} \right. \right\rangle \right) \quad (11)$$

are closely related to the ones in Tully’s paper [9, cf. Eqs. (10, 14)]; however, here they are calculated in terms of determinants of single-particle quantities. Note that B_{KL} is determined by a one-particle transition $\phi_{n_K} \rightarrow \phi_{n_L}$.

Comparing a uniform random number ξ between 0 and 1 to the values of (9) a transition from the current state K to K' takes place if $G_{K'-1} < \xi \leq G_{K'}$. These hopping events are gathered over a classical time step Δt (usually $\Delta t \gg \delta t$) and the last chosen state determines the force according to Eq. (8). By means of this method many-particle transitions are realized as subsequent one-particle transitions. In order to correct for the violation of the energy conservation (by $E_K - E_{K'}$) we rescale the atomic velocities $\dot{\mathbf{R}}_A$ along the coupling vectors

$$\mathbf{R}_A^{KK'} := \sum_{nn'} \sum_{\alpha\beta} f_n^K C_{n\alpha} \left(\mathbf{R}_{\alpha\beta}^A C_{\beta n'} + S_{\alpha\beta} \frac{\partial}{\partial \mathbf{R}_A} C_{\beta n'} \right) f_{n'}^{K'}. \quad (12)$$

Owing to the relatively high collision energy of 80 eV in the system under consideration (see next subsection) this is always possible.

The numerical effort of the procedure described above is only slightly higher for the system $\text{Na}_2^+ + \text{He}$ as compared to the usual NA-QMD approach [8], Eqs. (6) and (7). The matrix $C_{n\alpha}$ is interpolated over a classical time step and thus the time derivative in Eq. (11) is easily available. The derivative in (12) is done numerically and thus quite expensive. However, it is only required if a hopping event has occurred.

3.2 Results for $\text{Na}_2^+ + \text{He}$

In this section we present studies of $\text{Na}_2^+ + \text{He}$ collisions at $E_{\text{cm}} = 80 \text{ eV}$ based on the combination of the Tully surface hopping and the NA-QMD approach sketched in the

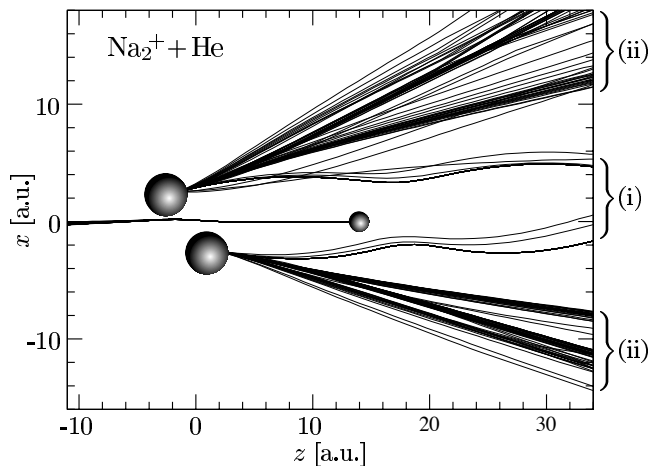


Fig. 2 Ensemble of trajectories of $\text{Na}_2^+ + \text{He}$ collisions at $E_{\text{cm}}=80\text{eV}$ for the very same collision geometry (depicted by the spheres) in the centre-of-mass system. The collision axis is along the z -axis with Na_2^+ flying from left to right and He from right to left.

previous section. This represents a first application of this formalism to a system which has been studied by conventional NA-QMD in detail [4]. Furthermore, experimental data from kinematically complete correlation experiments [5] are available for direct comparison.

At the collision energy considered here, two qualitatively different collision induced dissociation scenarios can be distinguished [4]: In the first case, named impulse mechanism, the helium atom transfers momentum to one sodium core resulting in vibrational excitation and subsequent fragmentation. The electronic mechanism, on the other hand, involves excitation of the molecule into a dissociative electronic state leading to the fragmentation owing to electron-vibrational coupling. Because we are interested in nonadiabatic effects, in the following, we concentrate on the latter one.

Firstly, we consider one fixed collision geometry. Figure 2 shows the collision plane of a central collision $\text{Na}_2^+ + \text{He}$ with an initial angle between molecule and collision axis of about 50° . Owing to the random hopping formalism, we obtain an ensemble of trajectories (each one of the 99 calculations gives three lines in Fig. 2) for the very same initial condition. This is in striking contrast to the conventional NA-QMD approach which is fully deterministic giving exactly one trajectory for one initial geometry.

Owing to the simplicity of the system, the structure of the trajectory ensemble (representing a classically sampled wave packet of the dissociation dynamics) can be understood in detail (see Fig. 2):

(i) Na_2^+ is only vibrationally excited due to a (small) momentum transfer to the sodium cores but it does not dissociate. The different trajectories resulted from occasional electronic excitation and subsequent deexcitations.

(ii) Na_2^+ is electronically excited to the $3s\sigma_u$, the $3p\sigma_g$, or the $3p\pi_u$ state leading to immediate fragmentation. The strong overlap in certain regions can be addressed to direct excitations to these states. The overall spread of the trajectories is caused

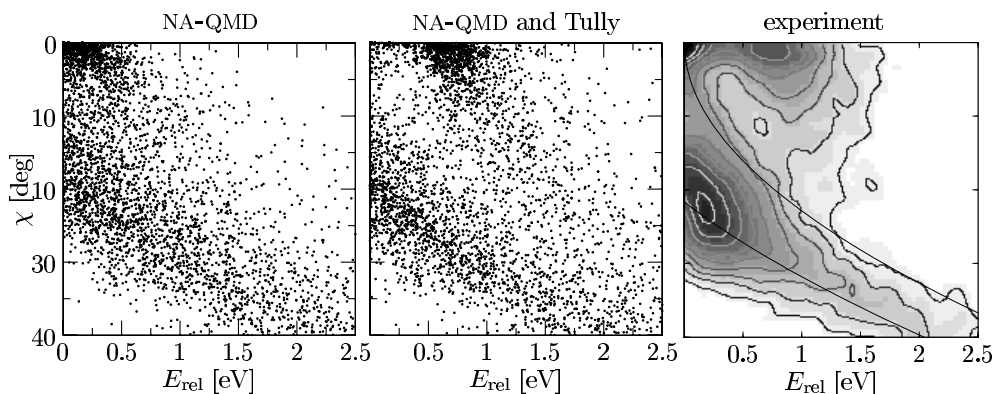


Fig. 3 Distribution of fragmentation events as a function of the relative energy of the fragments E_{rel} and the centre-of-mass scattering angle χ for $\text{Na}_2^+ + \text{He}$ at $E_{\text{cm}}=80$ eV. Calculations using NA-QMD (left) and the combination of NA-QMD and Tully surface hopping formalism (middle) are compared with the intensity plot (right) from kinematically complete experiments [5].

by excitation at different times and thus at different distances of the sodium atoms. Furthermore, multi-step excitations/deexcitations are not unlikely, resulting in a complicated hopping dynamics.

In order to compare with experimental data we have extended the analysis to randomly selected molecule orientations and all relevant impact parameters. Figure 3 shows the relative energy of the fragments E_{rel} and the centre-of-mass scattering angle χ of the projectile for all collision events that lead to fragmentation of the molecule (~ 4000 in the region shown out of 30 000 calculated collisions).

We restrict ourselves to the electronic dissociation events which can be found at small scattering angles $\chi \lesssim 10^\circ$. Whereas the NA-QMD calculations (left panel of Fig. 3) show *one* broad peak in this region the surface hopping approach (middle panel) clearly exhibits *two* peaks around $E_{\text{rel}} = 0$ and 0.7 eV in perfect agreement with the measurements (right panel). The scattering angle χ is almost the same in both calculations, see also the almost negligible impact of the hopping on the deflection of the (lightweight) He in Fig. 2. Obviously, quantum effects on the nuclear motion have only minor influence on the collision dynamics (at these impact energies) but can have dramatic implications on the relaxation (fragmentation) dynamics.

4 Summary and outlook

We have presented two approximate theories of wavepacket propagation. Evidently, both methods do have their favorite fields of application as well as inherent limitations. Molecular dynamics combined with surface hopping is, in particular, appropriate to describe situations where a large number of surfaces are coupled and therefore they must be calculated “on the fly”. Interference effects, however, are neglected in this

method. In contrast, semiclassical wavepacket propagation includes these effects, but its application to realistic systems is still restricted to situations where a limited number of well defined and previously calculated surfaces play a role.

One goal of future developments would be to combine the advantages of both methods, i.e. by including interference effects in molecular dynamics approaches as well as through the extension of semiclassical theories by calculating potential surfaces on the fly.

We would like to dedicate this paper to Peter Hänggi on the occasion of his birthday with all the best wishes for the future. Furthermore, FG would like to thank Gerhard Stock and Michael Thoss for valuable discussions on the mapping formalism and US and RS would like to thank Falk Richter for contributions to the numerical results for collision induced dissociation. Financial support by the Deutsche Forschungsgemeinschaft through the Forschergruppe "Nanostrukturierte Funktionselemente in makroskopischen Systemen" (FG and RS) and through a grant by the Deutscher Akademischer Austauschdienst and the Kungliga Vetenskapsakademien (US) is gratefully acknowledged.

References

- [1] A. Giusti-Suzor, F. H. Mies, L. F. DiMauro, E. Charron, and B. Yang, *J. Phys. B* **28** (1995) 309 and references therein
- [2] S. Chelkowski, T. Zuo, O. Atabek, and A. D. Bandrauk, *Phys. Rev. A* **52** (1995) 2977
- [3] T. Baumert, V. Engel, C. Meier, and G. Gerber, *Chem. Phys. Lett.* **200** (1992) 488
- [4] J. A. Fayeton, M. Barat, J. C. Brenot, H. Dunet, Y. J. Picard, U. Saalman, and R. Schmidt, *Phys. Rev. A* **57** (1998) 1058
- [5] J. C. Brenot, H. Dunet, J. A. Fayeton, M. Barat, and M. Winter, *Phys. Rev. Lett.* **77** (1996) 1246
- [6] G. Stock and M. Thoss, *Phys. Rev. Lett.* **78** (1997) 578
- [7] C. Meier, PhD thesis, University of Freiburg 1995
- [8] U. Saalman and R. Schmidt, *Z. Phys. D* **38** (1996) 153; *Phys. Rev. Lett.* **80** (1998) 3213
- [9] J. C. Tully, *J. Chem. Phys.* **93** (1990) 1061
- [10] M. F. Herman and E. Kluk, *Chem. Phys.* **91** (1984) 27
- [11] F. Grossmann, *Phys. Rev. A* **60** (1999) 1791
- [12] S. Magnier, Ph. Millié, O. Dulieu, and F. Masnou-Seeuws, *J. Chem. Phys.* **98** (1993) 7113
- [13] B. M. Garraway and K.-A. Suominen, *Rep. Prog. Phys.* **58** (1995) 365
- [14] N. Rosen and C. Zener, *Phys. Rev.* **40** (1932) 502
- [15] K.-A. Suominen, B. M. Garraway, and S. Stenholm, *Phys. Rev. A* **45** (1992) 3060
- [16] E. K. U. Gross and W. Kohn, *Adv. Quant. Chem.* **21** (1990) 255
- [17] A. Görling, *Phys. Rev. A* **54** (1996) 3912